PAPER NUMERICAL STUDY OF THE EFFECT OF WINDOW CONFIGURATION ON THE CONVECTIVE HEAT TRANSFER RATE OF A WINDOW

Meseret T. Kahsay [1], Girma Bitsuamlak[1], Fitsum Tariku[2]

[1] Department of Civil & Environmental Eng. /WindEEE Research Institute, University of Western Ontario

[2] Building Science Centre of Excellence, British Columbia Institute of Technology

ABSTRACT

In a cold winter, outdoor environmental conditions primarily influence the indoor surface temperature of building windows. This leads to a temperature gradient in the indoor environment which induces a downdraft affecting the thermal comfort of occupants. This phenomenon is sensitive to the configuration and location of windows. In this paper, the influence of window configuration on the convective heat transfer rate of a window is investigated numerically at different Rayleigh numbers of 1.7x106 to 1.7x1011. Convective heat transfer rate of a model window is evaluated using high-resolution 3-D steady Reynolds-Averaged Navier-Stokes (RANS) CFD simulations. Fluid properties have been assumed constant except for the density change with temperature which leads to the development of buoyancy force. The heater and the window are modeled as plane isothermal boundaries, the window being colder and the heater is hotter than the room air temperature. The sensitivity of window Nusselt number and room temperature distributions to various window configurations have been examined. Parameters investigated in this study include relative position of the heater from the window, the size of windows, and temperature of the heater. Results are discussed and compared with previous analytical, numerical and experimental works. Results of this study show that a window with horizontal configuration has the least rate convective heat transfer than that of vertical configuration.

Keywords: Computational Fluid Dynamics (CFD), steady RANS, turbulence modeling, window configuration, natural convection, Nusselt number.

INTRODUCTION

Globally, Canada is one of the largest energy consumers and space heating accounts for a remarkable 63% of the energy used in the average home, while in commercial and institutional settings, space heating accounts for 56% of all energy use (nrcan.gc.ca). This in large part is attributed to the thermal bridging caused by façade elements such as windows. In fact, 20 – 40% of energy in buildings is wasted through windows (Lee et al., 2013). Windows are configured in different forms as illustrated in Figure 1; hence,

proper design and selection of window system is regarded as one of the most important passive strategies for saving energy in buildings (Greenup & Edmonds, 2004; Tzempelikos, 2005; Ghisia et al., 2005; Ochoa et al., 2012).

Due to this, ASHRAE standard 90.1 (2010) provides a guideline on the Window-to-Wall Ratio (WWR) stating that: "the total vertical window area shall be less than 40% of the gross wall area". Although this is useful information, it does not account for differences in window configurations as well as the thermal and lighting performance for the same WWR. For example, consider the four window configurations illustrated in Figure 1 that have the same area of 20% WWR. It is important for, the guideline to accommodate as the question of which of the four window configurations is more energy efficient and thermally comfortable?

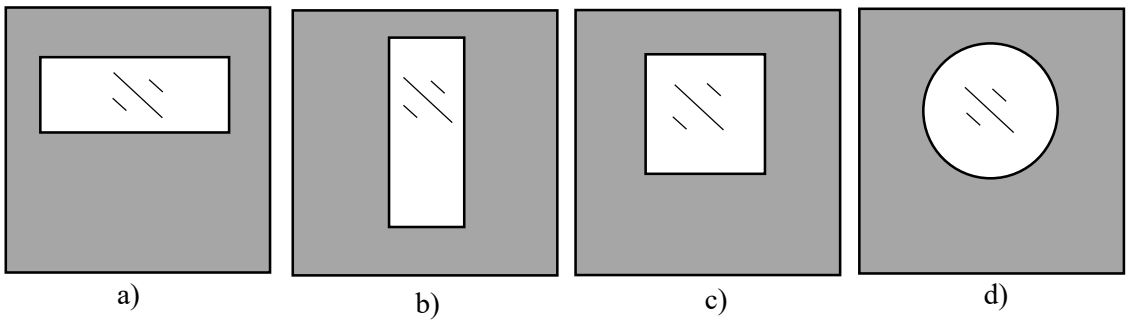

Figure 1: Model window configurations with 20% Window-to-Wall Ratio (WWR) that represent a) horizontal rectangular b) vertical rectangular c) square d) circular

To investigate the effect of different window configurations on the energy performance of a building, previous studies on the fundamentals of a vertical heated plate are examined including the following , experimental (Churchill & Chu, 1975), analytical (Eckert & Jackson, 1950) and numerical (Zitzmann et al., 2005) investigations. In addition to this, several studies of flow near window-wall heater systems have been investigated (Oosthuizen, 2011; Oosthuizen and Naylor, 2009). Although there have been many studies of flow near window-wall heater systems, most of these studies are two-dimensional and based on the assumption that the flow remains laminar and steady. There are limited studies that also consider both laminar and turbulent flows (Oosthuizen, 2011) and in most of the previous studies, only single window configuration was considered. Further, studies regarding the effect of different window configurations on convective heat transfer rate are very limited. Therefore, the present study investigates the influence of different window configurations on the indoor thermal discomfort and convective heat transfer rate of a window. Hence, an approximate numerical model of the convective heat transfer to a window below which a natural convective heater is mounted is considered to study how the relative window configurations and temperature of the heater affect the convective heat transfer rate of the window.

The remaining sections of the paper are organized as follows: section 2 provides validation of CFD simulations with previous experimental and computational studies on vertical isothermal planes. Section 3 describes details of the process and the parameters included in the computational fluid dynamics model. Section 4 presents result and discussion, and finally, section 5 concludes the paper.

VALIDATION OF CFD BASED NUSSELT NUMBER EVALUATION METHOD

Experimental Data for Validation

To validate the present numerical study, experimental data by Churchill and Chu (1975) for a flow over a vertical heated isothermal plate is used. In this experimental analysis, the Nusselt number for the entire Rayleigh number (Ra = 107-1012) from laminar, transition to turbulent natural convective regimes were evaluated.

The heat transfer rate from a vertical wall in the presence of turbulence in the boundary layer has been measured experimentally and correlated as a function, $(\overline{Nu}_y)(Ra_y, Pr)$, where $(\overline{Nu}_y)$ is the overall Nusselt number (Bejan, 2013). Based on their experimental data, Churchill and Chu (1975) constructed an empirical isothermal-wall correlation that reports the wall averaged Nusselt number $(\overline{Nu}_y)$ for the entire Rayleigh number as presented in Eq. 1.

$$(\overline{Nu}_y)=\{0.825+(0.387 Ra_y^{(1/6)})/[1+(0.492/Pr)^{(9/16)}]^{(8/27)}\}^2 \quad (1)$$

The physical properties used in the definition of $(\overline{Nu}_y)$, Ra_y, and Pr are evaluated at the film temperature $((T_w-T_a))/2$ where Tw is window temperature and Ta is air temperature (Bejan, 2013). The boundary layer flow remains laminar if y (height of window) is small enough so that the Rayleigh number Ra_y does not exceed a certain critical value. The transition to turbulent flow occurs at a y position where $Ra_y \sim 10^9$ Pr where Pr is Prandtl number. The Prandtl number is a ratio of viscosity diffusion rate to thermal diffusion rate ($Pr=(C_p \mu)/k$).

Numerical Model for Validation

In order to validate the wall-averaged Nusselt number with the empirical correlation of Churchill and Chu (1975), a computational domain (see Figure 2) that represents a two-dimensional heat transfer in a vertical isothermal window is used. In this study, the vertical right-side boundary was an open boundary and the inflow on this boundary has a constant air temperature of T_∞ (290 K). The wall was assumed to be adiabatic to isolate the window effects and the window was uniformly fixed at T_w (310 K) as shown in Table 1. The Nusselt number was evaluated for laminar, transition to turbulent regimes.

Table 1: Boundary conditions

Name	**Boundary Condition**
Wall	Adiabatic($u= v=0, q=0$)
Window	T_w = 310 K (isothermal)
Outlet	Pressure outlet, T_∞ = 290 K

u and v are velocities and q is a heat flux

In this study, a high-resolution, steady Reynolds-Averaged Navier-Stokes (RANS) CFD simulations using Shear Stress Transport (SST) k-w Low Reynolds number modeling (LRNM) approach has been used to resolve the near-wall heat transfer in conjunction with the buoyancy force. The buoyancy force is what causes the fluid motion in free convection. In addition, fluid properties are treated as constant values, except when changes in temperature lead to changes in density and the development of a buoyancy force. In other words, this scenario is treated using the Boussinesq approach.

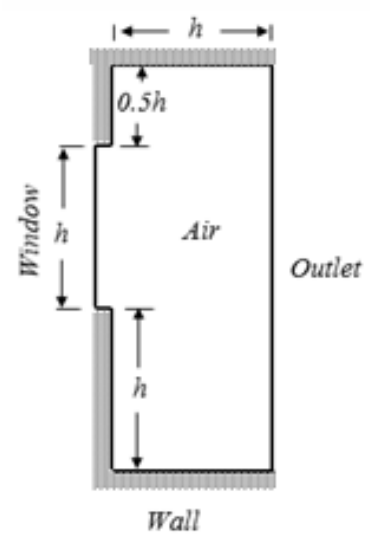

Figure 2: Model boundary conditions

The effect of the radiative heat transfer has been excluded. Thus, the solution is obtained by numerically solving the full two-dimensional governing equations. In this analysis, the height of the window, h, is used as the length scale and the magnitude of the overall temperature difference |(T_w-T_a)| is used as the temperature scale. The governing equations are (Eq. 2 - 4):

Continuity:

$$\partial u/\partial x+\partial v/\partial y=0 \tag{2}$$

Energy:

$$u\ \partial T/\partial x+v\ \partial T/\partial y=k/(\rho C_p\ )\ ((\partial\hat{}2\ T)/(\partial x\hat{}2\ )+(\partial\hat{}2\ T)/(\partial y\hat{}2\ )) \tag{3}$$

Momentum in the y-direction:

$$u\ \partial v/\partial x+v\ \partial v/\partial y=\vartheta\ (\partial\hat{}2\ v)/(\partial x\hat{}2\ )+\beta g(T-T_a\ ) \tag{4}$$

where C_(p)is specific heat capacity of air, β is volumetric thermal expansion coefficient, g is gravitational

acceleration, h is window height, and ϑ is kinematic viscosity of air.

Grid Sensitivity Analysis

The quality of the mesh has a significant effect on the accuracy of the results that are obtained from the simulation. Accordingly, the computational domain is discretized using polyhedral control volumes with a refined grid in the vicinity of the vertical heated plate (window) interior surfaces. Three levels of grid density with G1 (24,000 cells), G2 (34,090 cells), and G3 (52,400 cells) as illustrated in Figure 3 are used to assess the grid independence and to ensure that the optimum mesh size and computational accuracy for Low Reynolds Number Modeling (LRNM) simulations are met. The control volume is located close to the window where fine grids are deployed in order to capture important details of the temperature gradients and the flow structures.

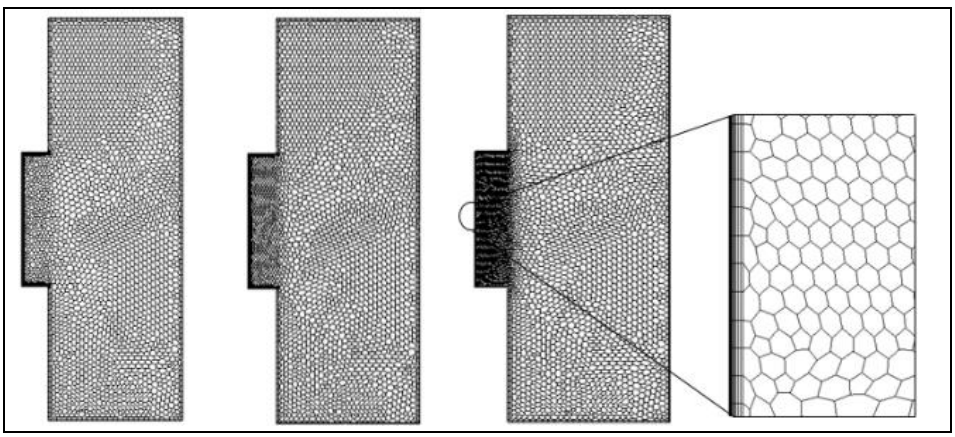

G1 G2 G3

Figure 3: Grid distribution resolution and sensitivity analysis

On the surfaces of the window, a viscous boundary layer with 10 grid layers is generated. A stretching factor of 1.05 is used to resolve the boundary layer at all solid-fluid interfaces of the control volume satisfying the recommendations of Franke et al. (2007) and Tominaga et al. (2008). To resolve this, the Low-Reynolds number modeling (LRNM), Shear Stress Transport k-ω (SST k-ω) turbulence model, has been used and it requires a very high grid resolution near the wall that is computationally expensive.

Accordingly, the simulation has employed a grid with cell centers at a minimum distance of 120 μm ($y+ < 5$) from the window surface to resolve the entire boundary layer, including the viscous sublayer and the buffer layer, that dominate the convective heat resistance. For a grid independence study of G1 (coarse), G2 (medium) and G3 (fine), the Nusselt number on the surface of the window is compared. The grid distribution of G3 (fine) confirmed that the simulated result does not change significantly as illustrated in Figure 4. Thus, the grid distribution of G3 has been adopted. Convergence is assumed when all the scaled residuals level off and reach the values 10-7 for x, y, z-momentum and energy, 10-5 for continuity and 10-6 for k and ε.

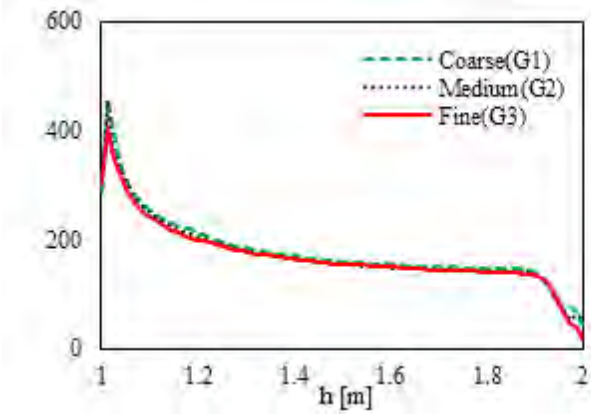

Figure 4: Grid sensitivity analysis: variation Nusselt number along height of the window

Comparison of CFD and Experimental Results

A computationally evaluated Nusselt number along a vertical centerline of a present study is compared with the experimental study of Churchill and Chu (1975) and previous computational results of Oosthuizen (2011) (Figure 5). Since the property of air is considered constant except for the density, the approximate value of property air (temperature, thermal conductivity, and specific heat capacity) is calculated for Pr = 0.7. The range of the study includes laminar cases that exist at lower Rayleigh number and turbulent flow at the higher Rayleigh number. The mean heat transfer from the window has been expressed in terms of the mean Nusselt number (Eq. 5), based on the reference window height.

$$[Nu]_w=((q_w^,)^{-} h)/k(T_a-T_w) \quad (5)$$

Where $(q_w^,)^{-}$ is the mean heat transfer rate from the window surface, h, is window height, k, is thermal conductivity of air, T_a , is room air temperature, T_w, window temperature, and the window Rayleigh number is expressed in the following Eq. 6 and 7.

$$Ra=Pr.Gr= (C_p \mu)/k ((\beta g(T_w-T_a)h^3)/\vartheta^2) \quad (6)$$

$$Gr=(\beta g(T_w-T_a) h^3)/\vartheta^2 \quad (7)$$

Where Gr is Grashof number, μ is the dynamic viscosity of air, h window height, and ϑ kinematic viscosity of air. As can be seen in Figure 5, the numerical results obtained in the present study for the case of a vertical heated window are in good agreement with experimental measurements of Churchill and Chu (1975) and previous numerical study of Oosthuizen (2011). The computational results match the experimental in the laminar region (Ra < 109). Beyond Ra > 109 (turbulent region), some discrepancy is noticed and increases with turbulence. The overall average deviation from the experimental result is less

than 10%. It is concluded that the results from CFD are reliable for a 2D simulation. Further, calibrated simulation is extended to a full-scale 3D computational section.

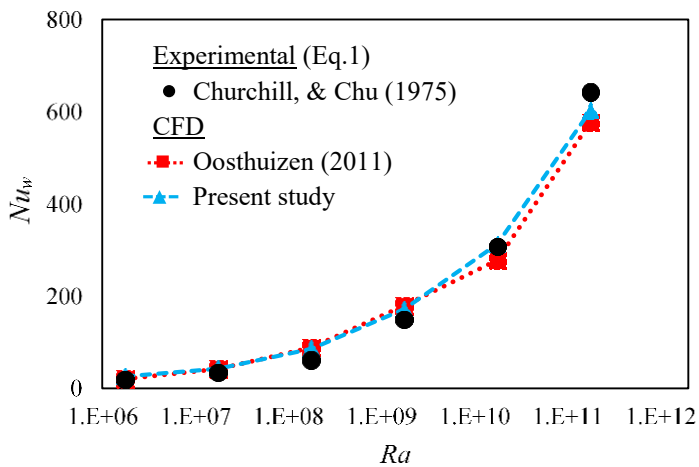

Figure 5: Comparison of experimental measured and numerical simulated window Nusselt number for various Rayleigh numbers.

CFD BASED EVALUATION OF CONVECTIVE HEAT TRANSFER RATE

Computational Domain

In this study, an office room of 4 m width, 3 m depth, and 2.5 m height is considered. Four different window configurations are evaluated with the same WWR of 20%. As illustrated in Figure 6, the heater width has been assumed to be greater than the window width which leads to a complex three-dimensional flow near the vertical edges of the window. The presence of the heater below the window alters the flow and temperature distributions. Hence, the main focus of this study is to investigate the lowest heater temperature that ensures the cold downward flow from the window is diverted away from the floor by the hot upward flow from the heater for different window configurations.

Boundary Condition

In this study only natural convection is considered. Thus, in a very basic way, to isolate the effect of window configuration on the room convective heat transfer rate, the heater and the window are modeled as plane isothermal boundaries, the window being colder and the heater is hotter than the room air temperature as shown in Table 2. Within the boundary conditions, the velocity is assumed to be zero on all the walls. The vertical right-side boundary is an open boundary, the inflow on this boundary is assumed to be a constant air temperature, T_a, and walls are assumed to be adiabatic. The dimensionless heater temperature (θ) is expressed as in Eq. 8.

$$\theta=((T_h-T_a))/((T_a-T_w)) \quad (8)$$

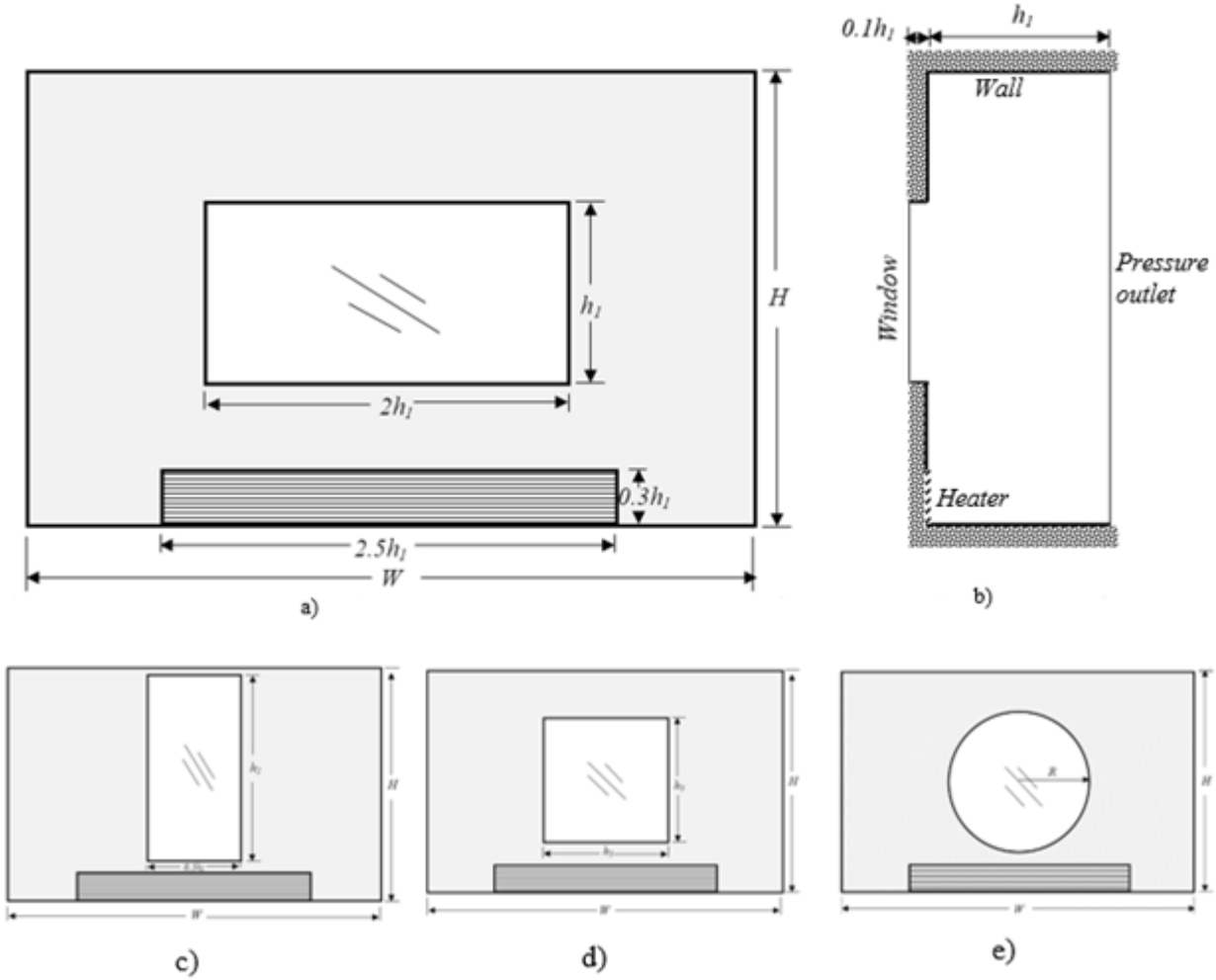

Figure 6: Model window used for parametric study a) horizontal configuration b) computational domain 2D representation c) vertical configuration d) square configuration, and e) circular configuration

Table 2: Boundary conditions

Name	**Boundary Condition**
Wall	Adiabatic($u= v=w=0,q=0$)
Window	Isothermal, $T_w = 283$ K
Heater	Isothermal, $T_h > T_a$
Outlet	Pressure outlet, $T_a = 294$ K

u, v, and w are velocities and q is heat flux

RESULTS AND DISCUSSION

In this section, the influence of window configuration on convective heat transfer will be discussed.

Case I: No convective heater below the window

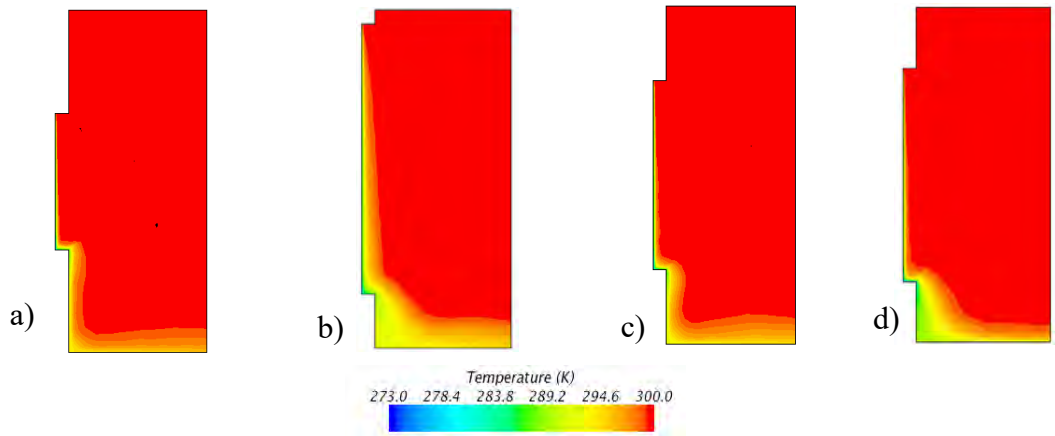

Figure 7: Plane section view of temperature contours for the case of a) horizontal b) vertical c) square d) circular where there is no heater for Raw = 109.

Figures 7 and 8 illustrates that due to the absence of the convective heater below the window, the air flows down from the cold window surface. Thus, the thickness of the air layer to which the vertical motion is confined increases from the top to the bottom. At a certain distance (see Figure 9), the airflow will become turbulent and increase in velocity near the floor.

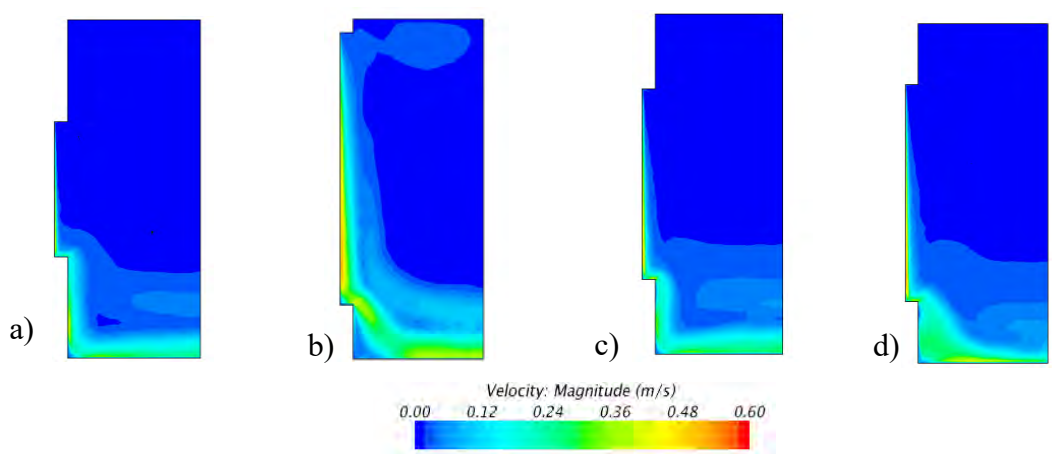

Figure 8: Plane section view of velocity contours for the case of a) horizontal b) vertical c) square d) circular where there is no heater for Raw = 109

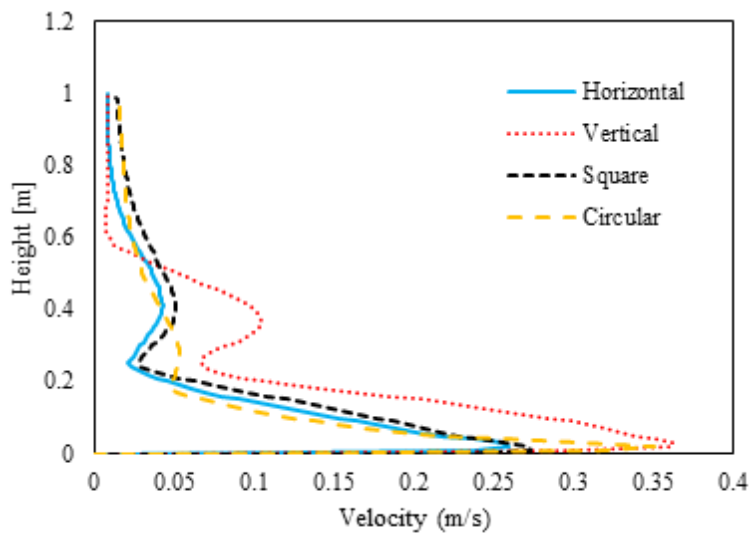

Figure 9: Case with no heater - Variation of downdraft velocity at a distance of 0.6 m (Ra = 1.7*109) (Standard, A. S. H. R. A. E., 2013)

In Figure 10 a-b, at lower values of Rayleigh numbers, the variation of the average Nusselt numbers are independent of the window configuration because the flow is laminar. However, at higher Rayleigh numbers, variations are dependent on the window configuration. Thus, comparing the average-Nusselt number value, the horizontal configuration shows the least and the vertical is the largest.

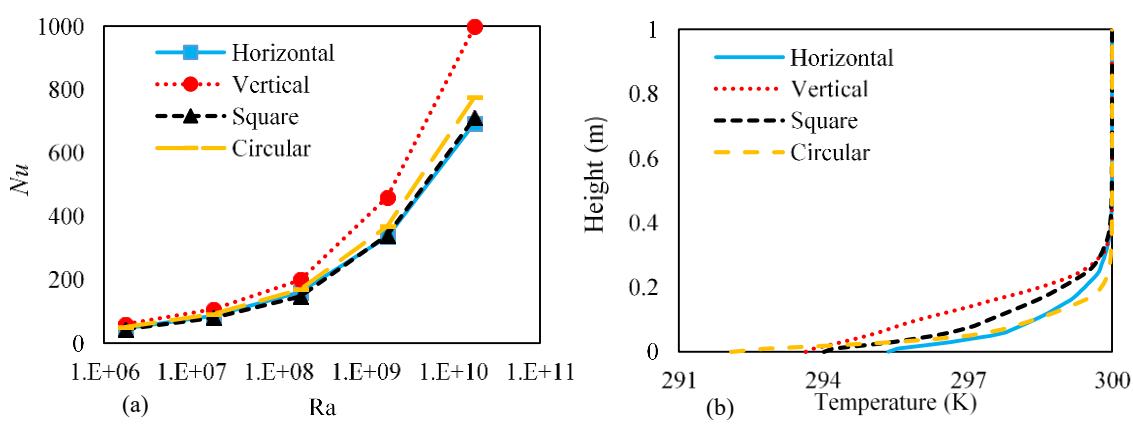

Figure 10: a) Variation of window Nusselt number with Rayleigh number for the case of no heater and b) variation of downdraft temperature at a distance of 0.6 m from the window for the case with no heater (Ra = 1.7*109) (Standard, A. S. H. R. A. E., 2013).

Case II: There is a convective heater below the window

For the case where there is a convective heater below the window, the solution parameters are 〖Ra〗_w and θ. The typical variations of window Nusselt numbers with Rayleigh number for dimensionless heater temperatures (θ) of 1, 2, 3, & 4 for four window configurations are presented. The mean heat transfer rate from the window has been expressed in terms of the average-Nusselt number (($\overline{〖Nu〗_w}$) (Eq. 5), based on the reference window height (h). At the lowest values of Ra (1.77×106 - 1.77*108) considered, the

windows Nusselt number variations are identical with the previous case where there is no heater below the window. However, at the higher values of Ra (1.77*109 - 1.77*1011) the window Nusselt numbers are higher due to the turbulent flow as illustrated in Figures 11 and 12.

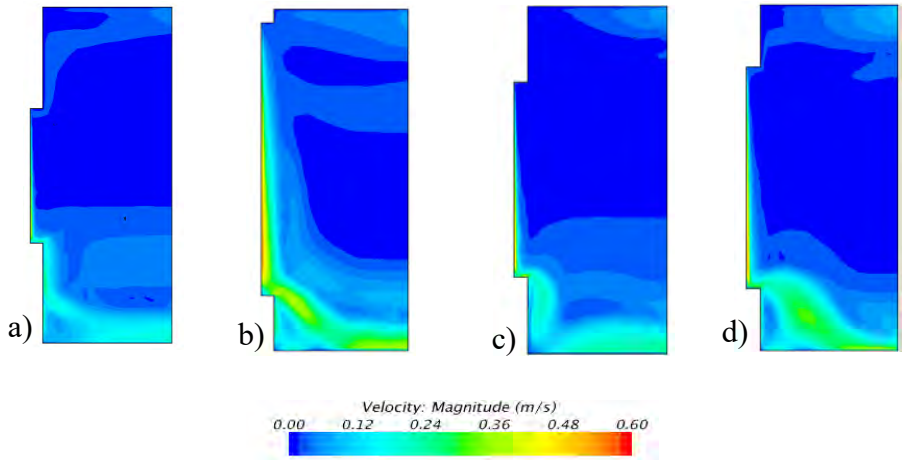

Figure 11: Plane section view of velocity contour for θ=1 and for the case of Ra =1.7*109 a) horizontal b) vertical c) square d) circular window configuration

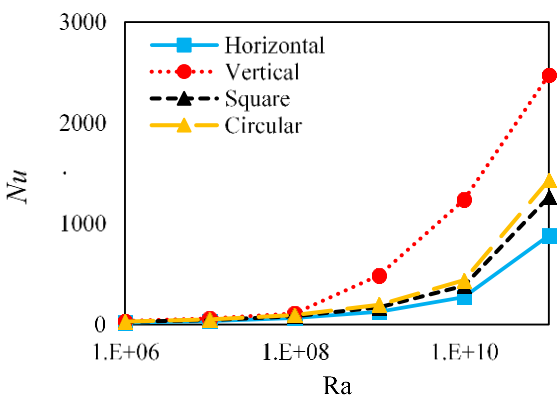

Figure 12: Variation of window Nusselt number with Rayleigh number for θ=1.

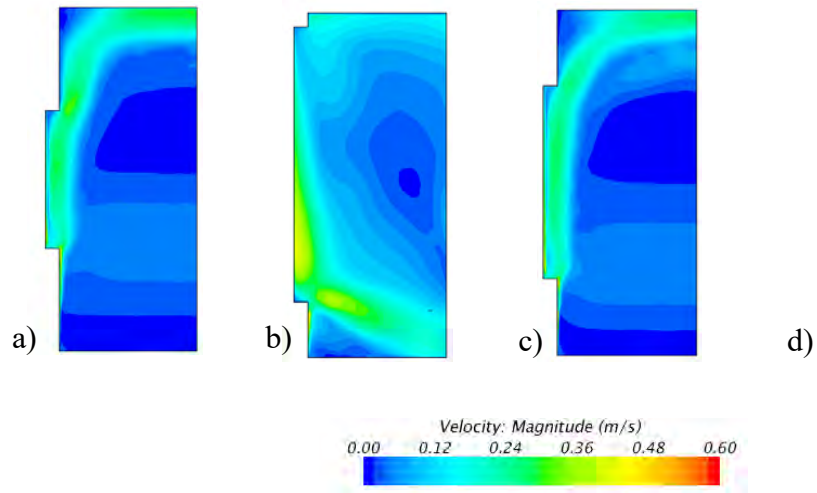

Figure 13: Plane section view of velocity contour for θ=4, and for the case of Ra =1.7*109 a) horizontal b) vertical c) square d) circular window configuration.

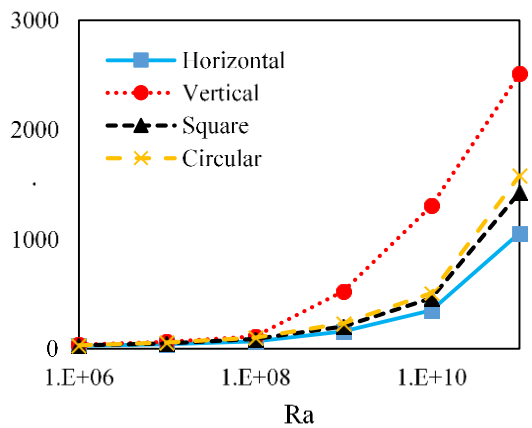

Figure 14: Variation of window Nusselt number with Rayleigh number for θ=4.

The changes in the direction (see Figure 13 and 14) of the flow are associated with the increasing θ. At low values of θ, the downward flow from the window dominates whereas at the higher values of θ the upward flow from the heater dominates. It is important to determine the minimum θ where the direction of the flow changes to maintain the thermal comfort of the room and save energy.

For the present case study, it is indicated that the flow direction change will occur at different θ for different window configurations. The flow changes from moving dominantly downward to dominantly upward for the entire Ra from 〖1.77*10〗^6-〖1.77*10〗^11 at a value of approximately θ=2, 4, 3, and 2.5 for horizontal rectangular, vertical rectangular, square and circular window configuration respectively. Therefore, as illustrated in Figure 15, comparing the convective heat transfer for each of the window configurations to achieve thermal comfort by diverting the down draft, the horizontal rectangular window configurations is the least. The vertical rectangular window configuration requires approximately double θ compared to the

horizontal window.

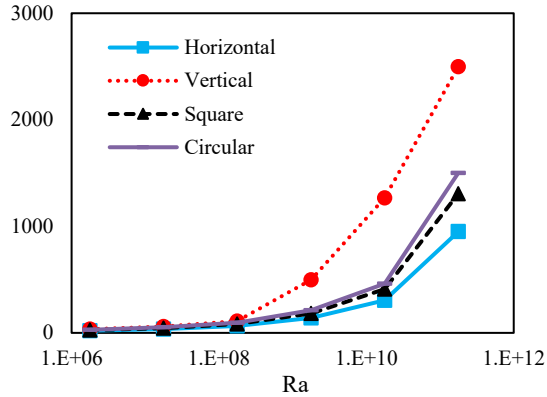

Figure 15: Variation of window mean Nusselt number with Rayleigh number averaged for a dimensionless heater temperature of θ=1, 2, 3, and 4.

In summary, considering the average windows Nusselt number as illustrated in Figure 15, at the lower values of Rayleigh number, the variations in convective heat transfer rate are independent of the dimensionless heater temperature (θ) and the window configuration. This is because the flow is laminar. However, at the higher values of Rayleigh numbers, the variations are dependent on the dimensionless heater temperature(θ), and the window configuration. Thus, the horizontal window configuration shows the least whereas the vertical shows the largest Nusselt number. Therefore, the horizontal window configurations perform better in terms of thermal comfort and the convective heat transfer rate.

CONCLUSION

This study evaluates four different window configurations, using high-resolution 3D steady RANS simulations of convective heat transfer at the internal surface of the window to determine the convective heat transfer rate. Initially, a CFD validation of the numerical model was carried out based on an experimental study of Churchill and Chu (1975) and numerical study of Oosthuizen (2011). The results of the CFD validation showed that LRNM of Shear Stress Transport k-ω models can provide accurate results for the convective heat transfer rate. Based on the validated computational procedures and techniques, convective heat transfer rate of a window was computed for full-scale models of different windows with and without convective heaters. Thus, the following conclusion have been deduced. Considering the window average-Nusselt number ($\overline{(Nu)}$), at the lower values of Rayleigh numbers (Ra), variations in convective heat transfer rate are independent of the window configuration and the dimensionless heater temperature (θ). This is because the flow is mainly laminar. However, at the higher values of the Rayleigh number, variations are dependent on the window configuration and the dimensionless heater temperature. Thus, the horizontal rectangular window configuration shows the least convective heat transfer rate value (Nusselt number) whereas the vertical rectangular configuration shows the largest convective heat transfer rate value.

The present study is limited to convective heat transfer aspects of the windows, but as part of the ongoing research, the authors are in the process of investigating the thermal comfort, daylighting and overall performance of the windows using a numerical approach. Along with the configuration of the window,

many other objectives will be considered that influence the energy consumption, thermal and lighting performance of the building, thus a multi-objective optimization analysis will be performed.

ACKNOWLEDGMENTS

The authors would like to thank SharcNet for providing access to their high-performance computing (HPC) facility and excellent support from their technical staff. The research support from Ontario Center of Excellence through Early Career Award to the first author and Canada Research Chair awards for both second and third authors are greatly appreciated.

REFERENCE

Bejan, A. (2013). Convection heat transfer. John Wiley & sons.

Churchill, S. W., & Chu, H. H. (1975). Correlating equations for laminar and turbulent free convection from a vertical plate. International journal of heat and mass transfer, 18(11), 1323-1329.

Eckert, E. R., & Jackson, T. W. (1950). Analysis of turbulent free-convection boundary layer on flat plate (No. NACA-TN-2207). National aeronautics and space administration Washington DC.

Franke, J., Hellsten, A., Schlünzen, H., Carissimo, B. (2007). "Best practice guideline for the CFD simulation of flows in the urban environment COST 2007." Action 732.

Ghisi, E., & Tinker, J. A. (2005). An ideal window area concept for energy efficient integration of daylight and artificial light in buildings. Building and environment, 40(1), 51-61.

Greenup, P. J., & Edmonds, I. R. (2004). Test room measurements and computer simulations of the micro-light guiding shade daylight redirecting device. Solar Energy, 76(1), 99- 109.

Handbook, A. S. H. R. A. E. (2009). Fundamentals, ASHRAE. Atlanta.

Lee, J. W., Jung, H. J., Park, J. Y., Lee, J. B., & Yoon, Y. (2013). Optimization of building window system in Asian regions by analyzing solar heat gain and daylighting elements. Renewable energy, 50, 522-531.

Machin, A. D., Naylor, D., Harrison, S. J., & Oosthuizen, P. H. (1998). Experimental study of free convection at an indoor glazing surface with a Venetian blind. HVAC&R Research, 4(2), 153-166.

National resources Canada, Heating Equipment. http://www.nrcan.gc.ca/energy/products/categories/heating/13740. Accessed Dec 24, 2016.

Ochoa, C. E., Aries, M. B., van Loenen, E. J., & Hensen, J. L. (2012). Considerations on design optimization criteria for windows providing low energy consumption and high visual

comfort. Applied Energy, 95, 238-245.

Oosthuizen, P. H., & Naylor, D. (1999). An introduction to convective heat transfer analysis. McGraw-Hill Science, Engineering & Mathematics.

Oosthuizen, P. H., Naylor, D. (2009). A numerical study of laminar-to-turbulent transition in the flow over a simple recessed window-plane blind system. In Proceedings of the 4th Canadian Solar Buildings Conference.

Oosthuizen, P. H., Naylor, D. (2010). A Numerical Study of the Effect of Blind Opening on Laminar-To-Turbulent Transition in the Flow over a Simple Recessed Window-Plane Blind System. In ASME 2010 International Mechanical Engineering Congress and Exposition (pp. 1487- 1493).

Oosthuizen, P. H., Paul, J. T. (2011). Numerical Study of the Convective Heat Transfer Rate from a Window Covered by a Top Down–Bottom Up Plane Blind System to an Adjacent Room. Chemical Engineering, 25, 749.

STAR CCM+. CD-ADAPCO product. (2015). www.cdadapco.com/products/star-ccm Accessed on Oct. 12, 2016.

SHARCNET is a consortium of colleges, universities and research institutes operating a network of high-performance computer clusters across south western, central and northern Ontario [Online]. Available: <www.sharcnet.ca>; 2016.

Standard, A. S. H. R. A. E. (2013). Standard 55-2013. Thermal environmental conditions for human occupancy.

Standard, A. S. H. R. A. E. (2010). ANSI/ASHRAE/IESNA Standard 90.1-2010. Energy standard for buildings except low-rise residential buildings.

Standard, A.S.H.R.A.E. (2014). ANSI/ASHRAE/USGBC/IES Standard 189.1-2014. Standard for the Design of High-Performance Green Buildings Except Low-Rise Residential Buildings.

Tominaga, Y., Mochida, A., Yoshie, R., Kataoka, H., Nozu, T., Yoshikawa, M., Shirasawa, T. (2008). "AIJ guidelines for practical applications of CFD to pedestrian wind environment around buildings." Journal of wind engineering and industrial aerodynamics, 96(10), 1749-1761.

Tzempelikos, A. (2005). A methodology for integrated daylighting and thermal analysis of buildings (Doctoral dissertation, Concordia University).

UNEP, United Nations Environment Program, http://www.unep.org/sbci/aboutsbci/background. asp. Accessed on Sep 11, 2016)

Zhang, Z., Zhang, W., Zhai, Z., and Chen, Q., 2007, "Evaluation of Various Turbulence Models in Predicting Airflow and Turbulence in Enclosed Environments by CFD: Part 2-Comparison with Experimental Data from Literature," ASME HVAC & R Research, 13(6), 871-886.

Zitzmann, T., Cook, M., Pfrommer, P., Rees, S., & Marjanovic, L. (2005, August). Simulation of steady-state natural convection using CFD. In Proc. of the 9th International IBPSA Conference Building Simulation 2005 (pp. 1449-1456). Montréal: IBPSA.